Enhanced Image Processing Pipeline and Parallel Generation of Multiscale Tiles for Web-based 3D Rendering of Whole Mouse Brain Vascular Networks

Jaerock Kwon
Department of Electrical and Computer Engineering, Kettering University, Flint, MI, U.S.A.

Keywords: Brain Vascular Networks, Knife-edge Scanning Microscope, Multi-scale Visualization.

Abstract: Mapping out the complex vascular network in the brain is critical for understanding the transport of oxygen, nutrition, and signaling molecules. The vascular network can also provide us with clues to the relationship between neural activity and blood oxygen-related signals. Advanced high-throughput 3D imaging instruments such as the Knife-Edge Scanning Microscope (KESM) are enabling the imaging of the full vascular network in small animal brains (e.g., the mouse) at sub-micrometer resolution. The amount of data per brain (for KESM) is on the order of 2TB, thus it is a major challenge just to visualize it at full resolution. In this paper, we present an enhanced image processing pipeline for KESM mouse vascular network data set, and a parallel multi-scale tile generation system for web-based pseudo-3D rendering. The system allows full navigation of the data set at all resolution scales. We expect our approach to help in broader dissemination of large-scale, high-resolution 3D microscopy data.

1 INTRODUCTION

The brain is foremost a heavily wired neuronal network, but there is also an intricate network of blood vessels that serves as an essential conduit for oxygen, nutrition, and various signaling molecules. The vascular network can also provide us with clues to the relationship between neural activity and blood oxygen level dependent (BOLD) signals in functional magnetic resonance imaging (fMRI) or near infrared spectroscopy (NIRS) signals. Thus, mapping out the full vascular network in the brain is an important challenge (Mayerich, Kwon, Sung, Abbott, Keyser, and Choe, 2011).

Advanced high-throughput 3D imaging instruments such as the Knife-Edge Scanning Microscope (KESM) enable the imaging of the full vascular network in small animal brains (e.g., the mouse) at sub-micrometer resolution. See Figure 1 for more details. This is sufficient to resolve the smallest capillaries (Mayerich *et al.*, 2011).

The amount of data produced by KESM imaging of the mouse brain is on the order of 2TB, thus it is a major challenge just to visualize it at full resolution.

To address this challenge, the KESM Brain Atlas (KESMBA) was developed (Chung, Sung, Mayerich, Kwon, Miller, Huffman, Abbott, Keyser, and Choe, 2011). This system is built on the Google Maps API, using multi-scale tiles with pseudo-3D rendering through transparent overlays. Figure 2 shows a screenshot of KESMBA.

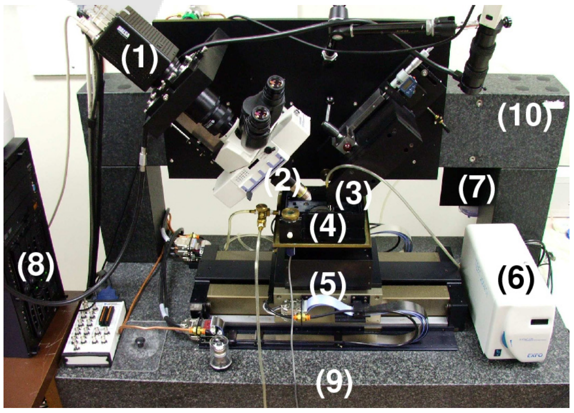

Figure 1: Knife-Edge Scanning Microscope (KESM). (1) high-speed line-scan camera, (2) microscope objective, (3) diamond knife assembly and light collimator, (4) specimen tank (5) three-axis precision stage, (6) white-light microscope illuminator, (7) water pump for the removal of sectioned tissue, (8) PC for stage control and image acquisition, (9) granite base, and (10) granite bridge.

Kwon J..
Enhanced Image Processing Pipeline and Parallel Generation of Multiscale Tiles for Web-based 3D Rendering of Whole Mouse Brain Vascular Networks.
DOI: 10.5220/0004926407830789
In *Proceedings of the 3rd International Conference on Pattern Recognition Applications and Methods* (ICPRAM-2014), pages 783-789
ISBN: 978-989-758-018-5
Copyright © 2014 SCITEPRESS (Science and Technology Publications, Lda.)
783

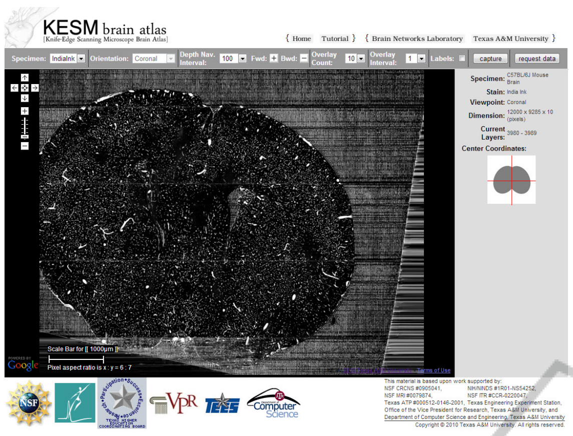

Figure 2: A screenshot of KESM Brain Atlas (KESMBA) (Chung et al., 2011).

However, the tile generation requires time-consuming manual calibration and the time required to download a single visualization is significant (~45 to 55 seconds/page for 20 overlays), requiring a lot of patience on the part of the user.

To address these two issues, we present an automated image processing pipeline for KESM mouse vascular images and a parallel multi-scale tile generation system for web-based pseudo-3D rendering that includes pre-overlaid tiles. The system, built on the OpenLayers API, allows full navigation and multi-scale viewing of the whole mouse brain data set at maximum resolution using a conventional web browser.

2 ENHANCED IMAGE PROCESSING PIPELINE

KESM employs physical sectioning imaging where thin slices of tissue are concurrently cut and imaged (Mayerich, Abbott, and McCormick, 2008). These slices are then re-assembled in order to produce the final volumetric data set (Kwon, Mayerich, Choe, and McCormick, 2008). In this section, we describe an enhanced image processing pipeline that performs the following tasks:

- The **Tissue Area Detector** detects the portion of the raw image that contains actual tissue data.
- The **Tissue Area Offset Corrector** identifies and corrects errors in the detected tissue area.
- The **Cropper** crops an image based on the corrected area information.
- The **Relighter** removes lighting artifacts and normalizes the inter-image intensity level.
- The **Merger** merges multi-column stacks into a large, single column image
- The **Overlay Composer** generates pre-overlaid images with a given number of images (e.g., an overlay of twenty 1μm-thick images will give a visualization a 20μm-thick slab) stack.
- The **Tiler** generates tile images for the web-based map service

In this paper, we provide details for the **Tissue Area Offset Corrector** and the **Overlay Composer**. The other phases of the pipeline have been described previously (Kwon, Mayerich, and Choe, 2011).

Automating the image processing steps is critical for generating brain atlases since the number of images is extremely large (e.g. 32,792 images in a whole mouse brain KESM data set). Previously, we automated key image processing steps including noise removal, image intensity normalization, and tissue area cropping (Kwon et al., 2008) (Kwon et al., 2011). However, the automation of several important steps remains, including correction of tissue area detection results. In addition, we demonstrate that pre-overlaying of images in the image stack is necessary to improve page load performance, and must also be automated.

2.1 Tissue Area Offset Corrector

The image processing pipeline starts from the Tissue Area Detector. A raw KESM image includes blank regions flanking the region that contains actual tissue data. Due to the physical sectioning process, the precise position of the tissue region in each image can show some variation due to repositioning of the knife or the objective during extended cutting/imaging sessions. We previously describe an automatic method for detecting the tissue region based on the right-most edge of the tissue (Kwon et al., 2011). However some images do not have a clear boundary due to uneven lighting across the knife edge. Failure to find a proper tissue boundary leads to incorrect cropping of the images, which are difficult to manually correct. Such errors impede proper reconstruction of 3D geometry in subsequent stages. However, we find that errors can be detected by observing the computed tissue region in adjacent images of the image stack. The sum of the difference between tissue area offsets in neighboring images is calculated. A sudden spike indicates an improperly detected tissue area offset. The summation continues until it reaches a certain threshold C:

$$S_n = \sum_{i=n}^{N} \Delta x_i \quad \text{until}\ \Delta x_i > C, \tag{1}$$

where S_n is the sum, $\Delta x_i = |x(i) - x(i-1)|$, and $x(i)$ is the tissue area offset of image i. The tissue area offset $x(i)$ is flagged as a spike (error) when S_n is less than the minimal chunk size R. A chunk is a stack of images that are obtained without any knife/objective repositioning, thus there should be no variation in $x(i)$. The $x(i)$ difference between two chunks is expected to be high. Once $x(i)$ is determined to be a spike, rather than the start of a new chuck, linear interpolation is applied to the spike. $x(i)$ will be replaced with $x(i-1)$. We used $C = 10$ and $R = 15$ in our case for (1). A simple spike can be removed by the approach described above. Yet several consecutive and irregular spikes cannot be removed in a single pass: One more round was required.

The summation of Δx_i continues until it reaches the maximum number of consecutive spikes (5 in our case) for the same data set. If the sum of differences is less than the mini- mum step size for a new chunk, the set of offsets $[x(i), x(i+1), \cdots]$ are labelled as spikes. Figure 3 shows initial tissue area offsets compared to the corrected offsets.

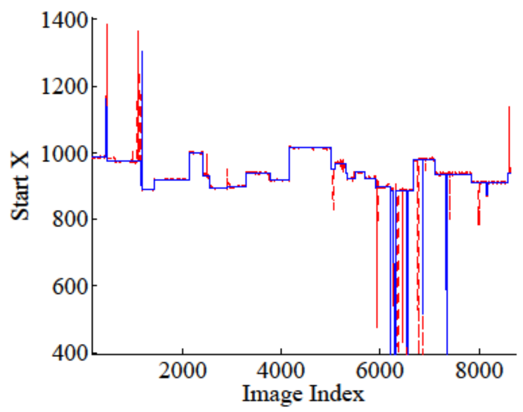

Figure 3: Correction of Improperly Detected Tissue Region. The red dashed lines show the original detection results. The blue solid lines indicate corrected results.

2.2 Overlay Composer

KESM produces images that represent a 1 mm-thick tissue section. This allows an unambiguous geometric reconstruction of the vascular network (i.e., there are no crossing or overlapping vessel segments in the image). Refer to Figure 4.

However, presenting one image at a time does not provide insights into the structural organization of the vascular network (Figure 5 (*a*)). Overlaying

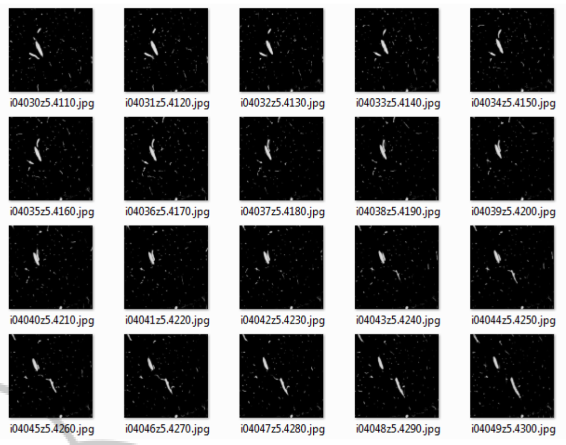

Figure 4: Series of Thinly Sliced Images. Structural Organization is hardly seen from a few series of images.

multiple images in the depth direction can overcome this limitation (Figure 5 (*b*)). In the current KESMBA, images with transparent background are downloaded on-the-fly and composed into an overlay by the web browser. However, the download time and overlay computation can be time-consuming. Furthermore, the addition of the required alpha channel incurs an extra overhead. Pre-computing the overlays is an effective alternative, and in this section we propose an efficient method that does not require this additional overhead. We first use (2) to pre-compute multiple overlays in an image stack:

$$\begin{aligned} O_n(x,y) &\leftarrow I_n(x,y) + \alpha_n \times I_{n+1}(x,y), \\ I_{n+1}(x,y) &\leftarrow O_n(x,y), \end{aligned} \tag{2}$$

where $O_n(x, y)$ is an intermediate output image after composing the n-th and $(n+1)$-th image, $I_n(x, y)$ is the n-th input image, and the index $n = 0\ (N - 1)$ where N is the number of overlay images. The attenuation factor α_n is defined in (3)

$$\alpha_n = \frac{(s - n \times r)^q}{s^q} \quad \text{where}\ n = 0 \ldots N-1, \tag{3}$$

where n is the depth index, N is the maximum depth, q is the order of the pixel intensity decrease rate, s is the initial value, and r is the attenuation rate. The values of the parameters were $s = 6$, $q = 2$, and $r = 0.1$. Figure 5 (*b*) shows an example of an overlay composed of 40 images created using the above method.

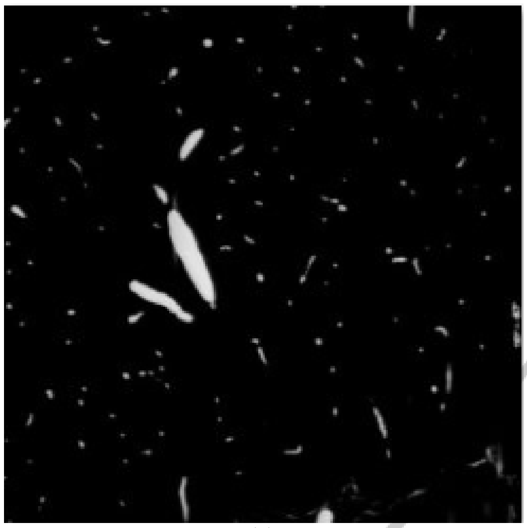
(*a*)

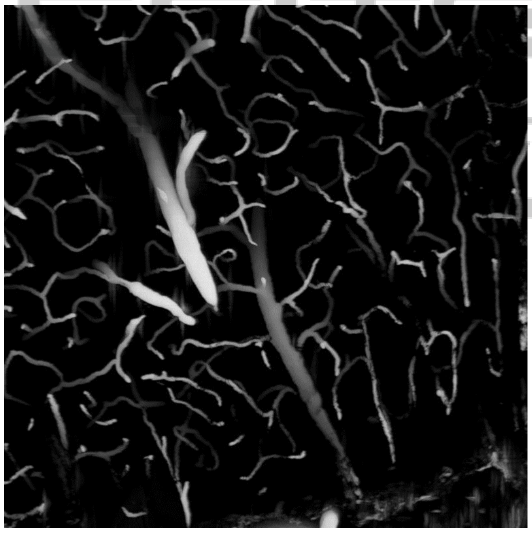
(*b*)

Figure 5: Transparent Overlay with Distance Attenuation. (*a*) A single KESM image (1 µm thickness). (*b*) An overlay of 40 KESM images (40 µm thickness), showing a local visualization of the vascular network. Objects in the foreground are brighter and those toward the background darker (distance attenuation).

3 PARALLELIZATION OF OVERLAY COMPOSER

Pre-overlaying images can greatly help reduce page load time for the KESM Brain Atlas, but preparing the pre-overlaid images (and map tiles) can be very time consuming. We need to process $O(10^4)$ very large images (12,000×9,600) and access more than 100 million pixels with each operation outlined in the previous section. On average, 1,203ms was needed to read a single image from a hard drive directly connected via USB 2.0. It took an average 10,046ms to compose two images to generate an intermediate overlay. The total time to read and compose 40 images to produce an intensity attenuation image was on average 1,203×40+10,046×39 = 439,914ms. The total number of images of the whole mouse brain vasculature data set is 9,628, thus it would take 1,177 hours (49 days) to complete the image composition on a single-core CPU.

Parallelization is a viable option in this case. We used commodity hardware to parallelize the pre-computation of overlays, without explicit parallel programming. The problems that need to be addressed are as follows: (*a*) Convenient deployment of image processing modules that are being actively developed (i.e., often updated) to all the workstations. (*b*) The ability to access the source data (the KESM image stack) and save the processed data. (*c*) Speed loss due to conflicts as more processes and workstations simultaneously access shared data resources.

3.1 System Design

To test performance gain due to parallelization, we designed a system utilizing node-level parallelism that does not require process-level or thread-level parallel programming. We built a network of connected workstations that share a Network Attached Storage (NAS). We made shared folders in the NAS and mapped them to network drives on the workstations so that image processing executables on the workstations can easily access the data sets. For data storage, DiskStation DS212j from Synology was used along with two hard disk drives; 2TB and 3TB. Five workstations were involved in the experiments. Each workstation had Intel Core i7 920 2.67GHz CPU and 6 GB of triple-channel PC10666 (1,333 MHz) RAM. There are two potential issues with this setup: (*a*) concurrent access to storage may degrade reading and writing performance, and (*b*) running multiple concurrent processes on each workstation can further complicate issue. We test these factors in the following section.

3.2 System Performance

Each process performs overlay composition. Initially, we tested the performance with a single process on a workstation directly attached to the NAS. We then increased the number of processes to 5, 10, ..., 30, and measured the performance. The number of workstations was also increased, from 1 to 5. The performance is measured by the total run time T, defined in (4).

$$T = \frac{(\gamma \times t_r + \beta \times t_c) \times N \times M}{p \times w}, \qquad (4)$$

Where t_r is the average time to read an image, t_c is the average time to compose an overlay of two images, N is the total number of layers (=40), M is the total number of images to be processed (=9,628), and p is the total number of processes. γ and β are time increment ratios in reading and composing images respectively as p increases, and w is the number of involved workstations. The overall experimental setup is described in Figure 6. Graphs in Figure 7 show the performance results.

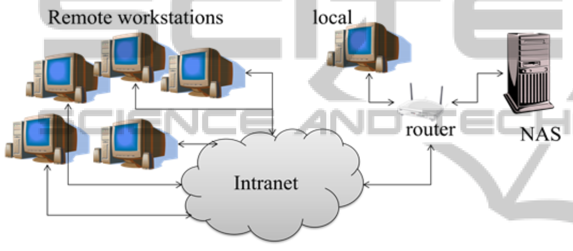

Figure 6: Overall Experimental Setup.

3.2.1 Single Workstation + USB

In this experiment, we varied the number of processes on a single workstation with the storage attached via USB. The sum of read time t_r (o) and overlay composition time t_c (×) per process increased by about three times, but the number of processors p was increased to 30, so the net performance gain is 10 times (in terms of reduction in T: +). We can conclude that using multiple processes is beneficial when the storage is local and concurrent access is enabled.

3.2.2 Single Workstation + NAS

We also investigated the case with a single workstation with a NAS. The results show that read time t_r(o) is decreased to the order of time required to produce the overlay t_c (×) when the NAS was accessed in parallel. Total processing time T (+) per process was increased six-fold, but the number of processes p increased to 30 so the net performance gain is 5 times (faster). With max p, the total processing can be done 10 times faster compared to the case where a single process is used.

3.2.3 Multiple Workstations (30 Processes)

Here we used up to 3 workstations running 30 processes each. The per workstation computation time T went up slightly less than two-fold, compared to the three-fold increase in the number of workstations w, thus the net reduction in computing time was 33%.

3.2.3 Multiple Workstations (5 Processes)

Here we used up to 5 workstations with fewer processes per workstation (=5). In this case, the per-workstation computing time went up four-fold, while the number of workstations w increases to five, distributing the load, thus it lead to a 28% reduction in computing time.

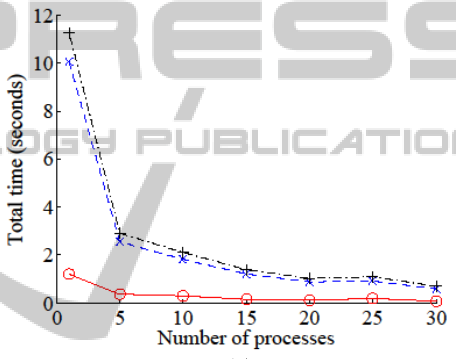

(a)

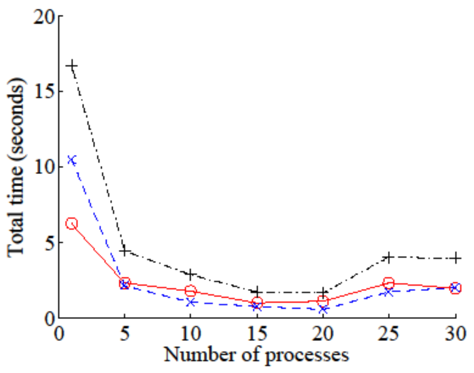

(b)

Figure 7: Processing Time. The wall-clock time for processing a 40-image overlay is shown for different server/process configurations. (a) Single workstation, number of process varied, USB-attached storage. (b) Single workstation, number of process varied, network-attached storage. (c) Multiple workstations, 30 processes per workstation, network-attached storage. (d) Multiple workstations, 5 processes per workstation, network-attached storage. The results show consistent performance gain, to a limit, as processes and nodes are added.

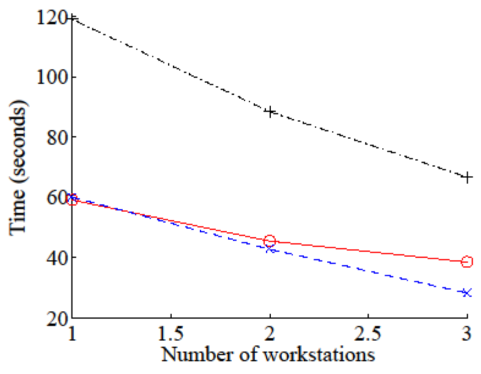

(*c*)

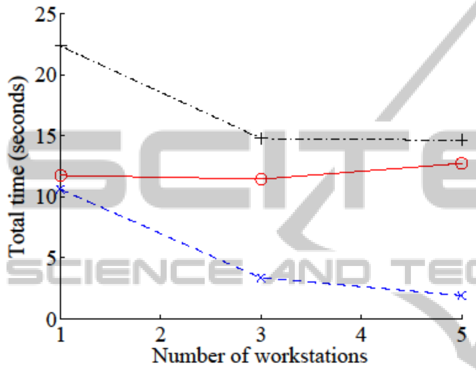

(*d*)

Figure 7: Processing Time. The wall-clock time for processing a 40-image overlay is shown for different server/process configurations. (*a*) Single workstation, number of process varied, USB-attached storage. (*b*) *S*ingle workstation, number of process varied, network-attached storage. (c) Multiple workstations, 30 processes per workstation, network-attached storage. (*d*) Multiple workstations, 5 processes per workstation, network-attached storage. The results show consistent performance gain, to a limit, as processes and nodes are added. (cont.)

4 ENHANCED KESM BRAIN ATLAS

To display and navigate the prepared multi-scale image tiles on a web browser we used OpenLayers, an open source web service platform. OpenLayers is an open map API that can display map tiles and markers. (Refer to http: //openlayers.org for more details.) The output of our image processing pipeline is a set of pre-overlaid images that is first converted into map tile images for OpenLayers.

4.1 Make Map Tiles with GDAL2Tiles

We used GDAL2Tiles to generate map tile images for OpenLayers. GDAL (Geospatial Data Abstraction Layer) (http://www.gdal.org) includes GDAL2Tiles that can generate map tiles for OpenLayers, Google Maps, Google Earth, and similar web maps. GDAL can be installed from OSGeo4W for Windows. (http://trac.osgeo.org/osgeo4w/). The following script can be used to create map image tiles from a single large image.

```
gdal gdal2tiles.py -p raster -z 0-6 -w
none filename.jpg
```

We created a script to process all image files in a folder as follows:

```
forfiles /m *.jpg /c "cmd /c gdal2tiles
-p raster -z 0-6 -w none @file"
```

Screenshots of the enhanced KESMBA is shown in Figure 8. All source code is accessible at https://github.com/jrkwon/KESMSuite.

5 CONCLUSIONS

In this paper, we presented an enhanced image processing pipeline for Knife-Edge Scanning Microscope mouse brain vasculature data. The pipeline included a Tissue Area Offset Corrector and Overlay Composer. We also proposed a parallelization system design and demonstrated its effectiveness. Finally, we built an OpenLayers-based web atlas based on the resulting images and tiles. Our approach is expected to be broadly applicable to large-scale microscopy data dissemination.

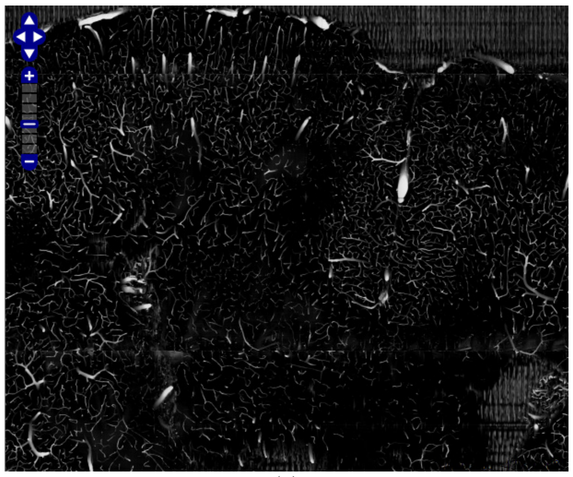

(*a*)

Figure 8: Enhanced OpenLayers-Based KESM Brain Atlas Screenshots of the enhanced KESMBA is shown. The mouse brain vasculature data set is shown at different scales.

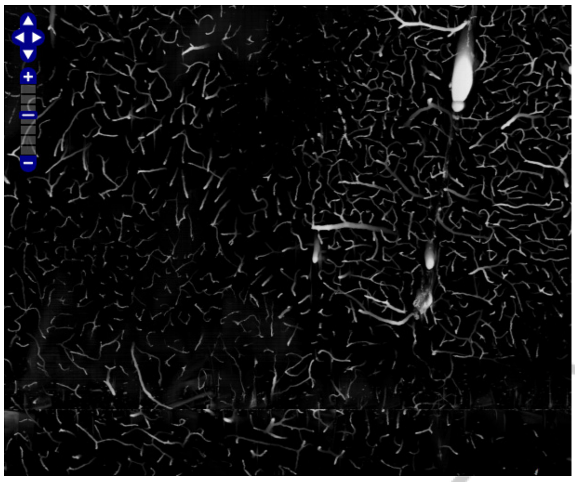
(b)

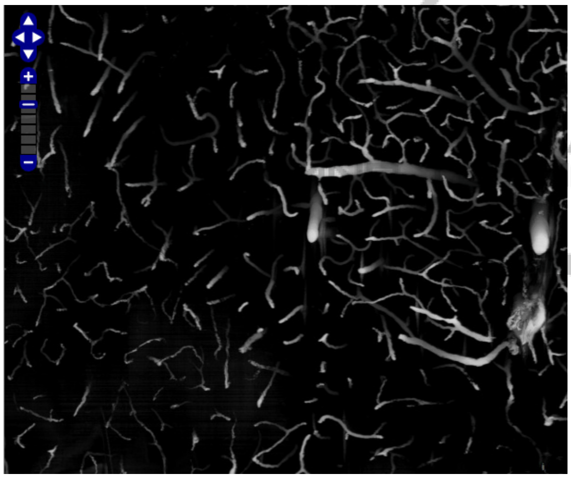
(*c*)

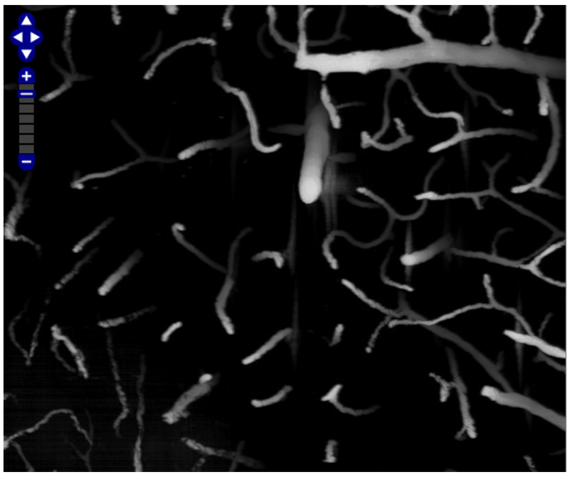
(*d*)

Figure 8: Enhanced OpenLayers-Based KESM Brain Atlas Screenshots of the enhanced KESMBA is shown. The mouse brain vasculature data set is shown at different scales. (cont.)

ACKNOWLEDGEMENTS

This publication is based in part on work supported by Award No. KUSC1-016-04, made by King Abdullah University of Science and Technology (KAUST); NIH/NINDS grant #R01-NS54252, NSF MRI #0079874; and NSF CRCNS #0905041 and #1208174. We would like to thank B. H. McCormick (KESM design), L. C. Abbott (tissue preparation), J. Keyser (graphics), and B. Mesa (KESM instrumentation).

REFERENCES

D. Mayerich, J. Kwon, C. Sung, L. C. Abbott, J. Keyser, and Y. Choe, “Fast macro-scale transmission imiging of microvascular networks using KESM,” *Biomedical Optics Express*, vol. 2, pp. 2888–2896, 2011.

J. R. Chung, C. Sung, D. Mayerich, J. Kwon, D. E. Miller, T. Huffman, L. C. Abbott, J. Keyser, and Y. Choe, “Multiscale exploration of mouse brain microstructures using the knife-edge scanning microscope brain atlas,” *Frontiers in Neuroinformatics*, vol. 5, pp. 29, 2011.

D. Mayerich, L. C. Abbott, and B. H. McCormick, “Knife-edge scanning microscopy for imaging and reconstruction of three-dimensional anatomical structures of the mouse brain,” *Journal of Microscopy*, vol. 231, pp. 134–143, 2008.

J. Kwon, D. Mayerich, Y. Choe, and B. H. McCormick, “Lateral sectioning for knife-edge scanning microscopy,” in *Proceedings of the IEEE International Symposium on Biomedical Imaging*, 2008, pp. 1371–1374.

J. Kwon, D. Mayerich, and Y. Choe, “Automated cropping and artifact removal for knife-edge scanning microscopy,” in *Proceedings of the IEEE International Symposium on Biomedical Imaging*, 2011, pp. 1366–1369.